
**Liquid Crystals**
Publication details, including instructions for authors and subscription information:
http://www.informaworld.com/smpp/title~content=t713926090

# Shear-induced rotations in a weakly anchored nematic liquid crystal

O. S. Tarasov[a]
[a] Institute of Molecule and Crystal Physics, Russian Academy of Sciences, 450075 Ufa, Russia

Online publication date: 21 May 2010

**To cite this Article** Tarasov, O. S.(2004) 'Shear-induced rotations in a weakly anchored nematic liquid crystal', Liquid Crystals, 31: 9, 1235 — 1240

**To link to this Article: DOI:** 10.1080/02678290410001729778

**URL:** http://dx.doi.org/10.1080/02678290410001729778

LIQUID CRYSTALS, VOL. 31, NO. 9, SEPTEMBER 2004, 1235–1240



# Shear-induced rotations in a weakly anchored nematic liquid crystal

O. S. TARASOV
†Institute of Molecule and Crystal Physics, Russian Academy of Sciences, 450075 Ufa, Russia
and Institute of Physics, University of Bayreuth, D-95440 Bayreuth, Germany

(*Received 19 February 2004; accepted 28 April 2004*)

We analyse the instability dynamics of a nematic liquid crystal under steady plane Couette flow. Weak anchoring for molecules of the nematic at the boundaries with an easy axis perpendicular to the flow plane is assumed. Orientation of the director along the easy axis is our basic state. Previously (Tarasov *et al.*, 2001, *Liq. Cryst.* **28,** 833), it was found that the critical shear rate of the primary instability of the basic state strongly decreases with anchoring strength. In the present study our interest was to examine the effect of the anchoring strength on the nematic dynamics in the regime with a slightly supercritical shear rate. It was found that for weaker anchoring the director rotates more strongly and the relaxation time of the amplitude of the basic state perturbations significantly increases. Results obtained can be used for experimental measurements of the anchoring strengths.



## 1. Introduction

Over recent decades, considerable efforts have been directed at examining the anchoring of liquid crystals (LCs) on solid surfaces with different morphologies. It is now widely known that the character of the surface interactions and LC ordering in the boundary layer strongly influence (if not determine) the bulk dynamic characteristics of the LC (orientation and relaxation/switching times), which are extremely important for optical devices [1, 2]. On the other hand, much less information is available on the role of the surface forces in pattern-forming instabilities, in particular, in the pattern selection. Patterns in LCs under a hydrodynamic flow, because of flow's ubiquitous character, are of special interest.

To extend our knowledge as to the role of anchoring conditions in hydrodynamic instabilities in LCs, we have turned to the dynamics of the (primary) homogeneous instability under steady plane Couette flow. The plane Couette flow is generated in a fluid between two parallel plates moving along the same axis with a certain constant velocity relative to each other. We concentrate on the case when the director at the bounding surfaces (substrates) is anchored perpendicularly to the flow plane, i.e. the plane spanned by the velocity of the primary flow and its gradient. For symmetry reasons, this orientation together with the linear velocity profile is the solution of the nematodynamic equations [3, 4] for any shear rate. This is our basic state. Such an orientation of the director is generally unstable, but may be stabilized by boundaries or external fields (for instance, a magnetic field) [5].

Experimentally, this system for the nematic MBBA has been investigated by Pieranski and Guyon [6, 7] in the 1970s, and more recently by Boudreau *et al.* [8]. It was found that the basic state loses stability when a flow with a critical shear rate $s_c$ is applied. For a zero or sufficiently weak magnetic field applied parallel to the initial director orientation, the homogeneous instability occurs. The type of instability changes to spatially periodic if the magnetic field is sufficiently strong [6]. In this case one observes rolls parallel to the flow direction. The mechanisms leading to the homogeneous or roll instabilities are generally well understood [6, 9]. The rolls are also observed in the absence of the magnetic field well above the threshold of the homogeneous instability [6]. The primary instabilities were investigated theoretically by Leslie [10] and Dubois-Violette and Manneville [9, 11–13]. The theoretical results were found to be in good agreement with the experiments of Pieranski and Guyon. Manneville has studied the dynamics of the director slightly above the threshold of the homogeneous instability [12]. He found that the director rotation is proportional to the overcriticality

*Author for correspondence; e-mail: tarasov@anrb.ru

*Liquid Crystals* ISSN 0267-8292 print/ISSN 1366-5855 online © 2004 Taylor & Francis Ltd
http://www.tandf.co.uk/journals
DOI: 10.1080/02678290410001729778

$\epsilon = [(s - s_c)/s_c]^{\frac{1}{2}}$, where $s$ is the shear rate. This has been confirmed experimentally [8].

One has to note that theoretical investigations have been performed under the assumption of strong anchoring of the director at the substrates. Recently, the homogeneous and spatially periodic instabilities in a NLC subjected to steady plane Couette or Poiseuille flow have been studied by means of a linear stability analysis in the case of weak director anchoring at the confining surfaces [14–16]. It has been established that the critical shear rate reduces with decreasing anchoring strengths. In the case of Poiseuille flow of the nematic MBBA the variation of the anchoring conditions can cause a crossover between two types of homogeneous or spatially periodic (roll) instabilities. In Couette flow of MBBA no such crossover was found, but the situation changes for slightly different material parameters [16]. These results are indicative of the strong influence of the anchoring conditions on the parameters of the instability and the pattern selection. In turn, a flow of oscillatory type was found to induce surface orientational transitions [17].

Here we focus on NLC dynamics slightly above the threshold of the homogeneous instability in steady Couette flow, taking into account anchoring conditions for the director. We formulate the problem mathematically in § 2. Starting from the well known Ericksen–Leslie equations [3, 4], we define the expansion scheme and derive the equation for the amplitude of the director and fluid velocity perturbations from the basic state in § 3. In § 4 the data on the relaxation time of the perturbation amplitude and the rotation of the director as functions of the anchoring strengths are presented and compared with available experimental findings. We discuss the results and conclude in § 5.

## 2. Formulation of the problem

We consider a NLC layer of thickness $d$ sandwiched between two parallel infinite plates. The origin of a Cartesian coordinate system is placed at the centre of the layer with the $z$-axis perpendicular to the bounding plates. Steady Couette flow is generated by one plate (at $z = d/2$) moving with constant velocity $V^0$ along the $x$-direction and the other plate (at $z = -d/2$) fixed. The spatially constant shear rate is $s = V^0/d$.

The confining plates provide the preferable director orientation $\mathbf{n}^0$ along the $y$-axis (easy axis). In the case of small director deviations $\hat{\mathbf{n}} = \mathbf{n} - \mathbf{n}^0$ at the substrates, the energy costs of the distortion can be described by the potential

$$F_s = \frac{1}{2} W_a \hat{n}_x^2 + \frac{1}{2} W_p \hat{n}_z^2, \quad W_a > 0, \quad W_p > 0 \quad (1)$$

where $W_p$ is a 'polar' anchoring strength related to out-of-substrate-plane director deviations and $W_a$ is an 'azimuthal' anchoring strength related to deviations within the substrate plane.

The boundary conditions for the director perturbations $\hat{\mathbf{n}}$ can be obtained from the surface torque balance equation

$$\pm K_{22} \hat{n}_{x,z} + \frac{\delta F_s}{\delta \hat{n}_x} = 0, \quad \pm K_{11} \hat{n}_{z,z} + \frac{\delta F_s}{\delta \hat{n}_z} = 0, \quad \text{for } z = \pm d/2. \quad (2)$$

Here $K_{11}$ and $K_{22}$ are splay and twist elastic constants, respectively. The notation $f_{,z} = \partial f / \partial z$ is used.

The basic state is given by the stationary homogeneous solution of the standard set of the nematodynamic equations [3, 4]

$$\mathbf{n}^0 = (0, 1, 0), \quad \mathbf{v}^0 = \left(v_x^0, 0, 0\right) \quad (3)$$

where $v_x^0 = V^0(1/2 + z/d)$.

In what follows we consider the temporal evolution of homogeneous perturbations to the solution (3) in the form

$$\mathbf{n} = \mathbf{n}^0 + \left(\hat{n}_x, \hat{n}_y, \hat{n}_z\right), \quad \mathbf{v} = \mathbf{v}^0 + \left(\hat{v}_x, \hat{v}_y, \hat{v}_z\right) \quad (4)$$

where $\hat{n}_i$ and $\hat{v}_i$ ($i = x, y, z$) are functions of coordinate $z$ and time $t$. One notes, that in the homogeneous problem, only $x$ and $z$ components of the director perturbations and the $y$ component of the velocity perturbations are relevant. The equations for the other components remain uncoupled. Moreover, from the normalization condition $\mathbf{n}^2 = 1$ one has $\hat{n}_y = 0$. Let us introduce the dimensionless quantities

$$\tilde{z} = \frac{z}{d}, \quad \tilde{t} = \frac{t}{\tau_d}, \quad S = \beta \tau_d s,$$
$$V_y = \frac{\beta^2 b \tau_d}{d} \hat{v}_y, \quad N_x = \beta \hat{n}_x, \quad N_z = \hat{n}_z \quad (5)$$

with

$$\beta^2 = \frac{\alpha_3}{\alpha_2} \frac{K_{22}}{K_{11}} \frac{1}{b}, \quad b = \frac{\eta_1}{\eta_3} \quad (6)$$

and orientational and viscous characteristic times

$$\tau_d = \frac{(-\alpha_2) d^2}{K_{22}}, \quad \tau_v = \frac{\rho d^2}{\eta_3}. \quad (7)$$

Here $\eta_1 = (\alpha_3 + \alpha_4 + \alpha_6)/2$, $\eta_3 = \alpha_4/2$, $\rho$ is the mass density of the nematic, $\alpha_i$ are Leslie coefficients related to viscosity and $K_{ii}$ are elastic constants. It is useful to note that for the material parameters of MBBA [18] and $d = 150\,\mu\text{m}$ (parameters of the experiment [8], see below) the orientational relaxation time $\tau_d \approx 6\times10^2$ s, while $\tau_v \approx 6\times10^{-4}$ s.†

It is convenient to express the shear rate as

$$S = a^2, \; a^2 = \frac{V^0 \tau_d}{d}\beta. \tag{8}$$

Further, the boundary conditions (2) and no-slip boundary condition for the fluid velocity reduce to

$$\begin{aligned} \pm N_{x,z} + w_a N_x &= 0 \\ \pm N_{z,z} + w_p N_z &= 0 \\ V_y &= 0 \end{aligned} \tag{9}$$

at $z = \pm 1/2$, where the dimensionless quantities

$$w_a = W_a d / K_{22}, \quad w_p = W_p d / K_{11} \tag{10}$$

are introduced. In the limit of strong anchoring ($w_a$, $w_p \to \infty$) one has $N_x = N_z = 0$ at $z = \pm 1/2$, whereas for torque-free boundary conditions ($w_a$, $w_p \to 0$) $N_{x,z} = N_{z,z} = 0$ at the boundaries. Since experimental measurements show $W_p$ changing from $10^{-7}$ to $10^{-3}\,\mathrm{J\,m^{-2}}$ [19], the dimensionless quantity $w_p$ is ranged from 4 to $4\times10^4$ for $d = 150\,\mu$m and MBBA material parameters [18]. Azimuthal anchoring strength $W_a$ and, consequently, its dimensionless relative $w_a$ are at least one order of magnitude smaller [19].

## 3. Analysis

Using expressions (4), the system of nematodynamic equations [3, 4] can be written in the form

$$\frac{\partial}{\partial t}\mathbf{x} = \mathcal{L}(S)\mathbf{x} + \mathbf{h}(\mathbf{x}, S) \tag{11}$$

where $\mathbf{x} = (N_x, N_z, V_y)^T$, $\mathcal{L}$ is a linear differential operator, the shear rate $S$ represents the control parameter and $\mathbf{h}$ is a non-linear part.

Renormalizing the velocity as $V_y = (1-b)Y$ [12] the linear operator can be written

$$\mathcal{L} = \begin{pmatrix} S & \partial_{zz} & 0 \\ \partial_{zz} & bS & (1-b)S\partial_z \\ 0 & -(1-b)S\partial_z & -(1-b)S\partial_{zz} \end{pmatrix} \tag{12}$$

where $\partial_z \equiv \partial/\partial z$ and so on. Then the linear operator becomes self-adjoint $\mathcal{L} = \mathcal{L}^+$.

Introducing a small parameter $\epsilon = [(S - S_c)/S_c]^{\frac{1}{2}}$, we define the expansion

$$\begin{aligned} \mathbf{x} &= \epsilon\mathbf{x}^{(1)} + \epsilon^2\mathbf{x}^{(2)} + \epsilon^2\mathbf{x}^{(3)} + \ldots \\ S &= S_c + \epsilon S_1 + \epsilon^2 S_2 + \epsilon^3 S_3 + \ldots. \end{aligned} \tag{13}$$

†MBBA material parameters at 25°C [18]. Elastic constants, $10^{-12}$ N: $K_{11} = 6.66$, $K_{22} = 4.2$, $K_{33} = 8.61$. Viscosities, $10^{-3}\,\mathrm{N\,s\,m^{-2}}$: $\alpha_1 = -18.1$, $\alpha_2 = -110.4$, $\alpha_3 = -1.1$, $\alpha_4 = 82.6$, $\alpha_5 = 77.9$, $\alpha_6 = -33.6$. Mass density $\rho = 10^3\,\mathrm{kg\,m^{-3}}$.

The critical slowing down inherent to the theory of critical phenomena [20] suggests introducing relevant time scales through

$$\frac{\partial}{\partial t} = \epsilon\frac{\partial}{\partial \tau_1} + \epsilon^2\frac{\partial}{\partial \tau_2} + \ldots \tag{14}$$

Substituting equations (13) and (14) into (11) one gets at the first order in $\epsilon$ the linear problem

$$\mathcal{L}(S_c)\mathbf{x}^{(1)} = 0. \tag{15}$$

The general solution of equation (15) is

$$\mathbf{x}^{(1)} = A(\tau_1, \tau_2, \ldots)\mathbf{u} \tag{16}$$

where $A$ is an amplitude, as yet undetermined, and $\mathbf{u}$ is the eigenvector obtained in [14], as well as the critical shear rate $S_c = a_c^2$. We give for reference the solution of the linear problem corresponding to the relevant *even* (symmetric) type (see [14] for details):

$$\begin{aligned} N_x &= m_p\cosh(a_c z) + \cos(a_c z) - \\ &\quad - w_a^{-1}[w_a\cosh(a_c/2) + a_c\sinh(a_c/2)] \\ &\quad (m_p + m_a) \\ N_z &= -m_p\cosh(a_c z) + \cos(a_c z) \\ (1-b)\,Y &= m_p(1-b)a_c\sinh(a_c z) + (1-b)a_c\sin(a_c z) + \\ &\quad + w_a^{-1}[w_a\cosh(a_c/2) + a_c\sinh(a_c/2)] \\ &\quad (m_p + m_a)a_c^2 bz. \end{aligned} \tag{17}$$

with

$$m_{p(a)} = \frac{w_{p(a)}\cos(a_c/2) - a_c\sin(a_c/2)}{w_{p(a)}\cosh(a_c/2) + a_c\sinh(a_c/2)}. \tag{18}$$

We retain, in the following, the notation for the components of the linear problem solution as in equations (17).

From the analysis of the equations at the second order it follows that $S_1 = 0$, $\partial A/\partial\tau_1 = 0$ and $\mathbf{x}^{(2)} = 0$. Then, one may choose $S_2 = S_c$ and one obtains at the third order in $\epsilon$

$$\mathcal{L}(S_c)\mathbf{x}^{(3)} = \mathbf{q}^{(3)}. \tag{19}$$

Clearly, the solvability condition

$$\langle \mathbf{u}^+, \mathbf{q}^{(3)} \rangle = 0 \tag{20}$$

has to be satisfied, where $\mathbf{u}^+$ is the solution of the adjoint problem

$$\mathcal{L}^+(S_c)\mathbf{u}^+ = 0 \tag{21}$$

and the scalar product $\langle a, b\rangle = \int_{-1/2}^{1/2} ab\,\mathrm{d}z$. Since the linear operator $\mathcal{L}$ is self-adjoint, one has $\mathbf{u}^+ = \mathbf{u}$. The solvability condition (20) yields the equation for the amplitude $A$.

The components of the inhomogeneity $\mathbf{q}^{(3)}$ in equation (19) are given by

$$\begin{aligned}
\mathbf{q}_1^{(3)} &= -AS_cN_z + A^3p_1 + A_{,\tau_2}(1-\lambda)N_x \\
\mathbf{q}_2^{(3)} &= -AbS_cN_x + A^3p_2 + A_{,\tau_2}\frac{1-\lambda}{\lambda}\beta^2 bN_z \\
\mathbf{q}_3^{(3)} &= A(1-b)S_cN_{x,z} + A^3p_3 + A_{,\tau_2} \\
&\quad \left\{(1-b)\frac{\tau_v}{\tau_d}S_cY - \alpha_3'\beta^2 N_{z,z}\right\}
\end{aligned} \tag{22}$$

with

$$\begin{aligned}
p_1 &= (1-k_{32})\left(N_z^2N_{x,z}\right)_{,z} - N_x\left(\frac{1}{\beta^2}N_{x,z}^2 + N_{z,z}^2\right) - \\
&\quad -\frac{1}{\beta b}N_zV_{x,z}^{(2)} - \left[1-k_{12}+\frac{1-\lambda}{\beta^2 b}\right]N_xN_zN_{z,zz} \\
p_2 &= \frac{1}{\beta_2}(k_{31}-2k_{21})N_{x,z}^2N_z - \frac{1}{\beta}N_xV_{x,z}^{(2)} - k_{31}N_zN_{z,z}^2 + \\
&\quad +\frac{1}{2}(1-b)S_c\left(\frac{1}{\beta^2}N_x^2+N_z^2\right)Y_{,z} \\
&\quad +\left[1-k_{31}-\frac{1+\lambda}{\lambda}\right]N_{z,zz}N_z^2 \\
p_3 &= \frac{1-b}{\beta b}\left(N_xV_{x,z}^{(2)}\right)_{,z} - \frac{(1-b)^2}{\beta^2 b}S_c\left(N_x^2Y_{,z}\right)_{,z} - \\
&\quad -\frac{1}{2}\left[1-b+2\alpha_1'\right]S_c\left(N_z^2N_x\right)_{,z} - \\
&\quad -\left(\alpha_2'+\alpha_3'-\alpha_1'\right)(1-b)b^{-1}S_c\left(N_z^2Y_{,z}\right)_{,z} \\
&\quad -\frac{1}{2}\frac{1-b}{\beta^2}S_c\left(N_x^3\right)_{,z}
\end{aligned} \tag{23}$$

where $(N_x, N_z, Y)$ are from equations (17), $\eta'_i = \eta_i/\eta_3$, $\alpha'_i = \alpha_i/\eta_3$, $\lambda = \alpha_3/\alpha_2$ and $k_{ij} = K_{ii}/K_{jj}$. The velocity $V_x^{(2)}$ can be found from the uncoupled $x$ component of the Navier–Stokes equation at the second order in $\epsilon$:

$$V_{x,z}^{(2)} = C_0 - \frac{1-b}{\beta}N_xN_{z,zz} - \beta bS_c\left(\eta_2'-1\right)N_z^2. \tag{24}$$

The coefficient $C_0$ is determined from boundary conditions for the velocity $V_x^{(2)}(z=\pm 1/2)=0$:

$$C_0 = \frac{1-b}{\beta}\int_{-1/2}^{1/2}N_xN_{z,zz}\,dz + \beta bS_c\left(\eta_2'-1\right)\int_{-1/2}^{1/2}N_z^2\,dz. \tag{25}$$

Introducing a new amplitude $B=\epsilon A$ from the solvability condition (20) one gets

$$\tau_B B_{,t} = \frac{S-S_c}{S_c}B - gB^3. \tag{26}$$

The amplitude equation (26) is the central result of the present study. The coefficients in equation (26) are expressed via

$$\tau_B = \frac{a_1}{a_2}, \quad g = \frac{a_3}{a_2} \tag{27}$$

with

$$\begin{aligned}
a_1 &= (1-\lambda)(1+k_{21})\langle N_x, N_z\rangle - \\
&\quad -(1-b)\frac{\tau_v}{\tau_d}S_c\langle Y, Y\rangle - \alpha_3'\beta^2\langle Y, N_{z,z}\rangle \\
a_2 &= S_c\langle N_z, N_z\rangle + b\langle N_x, N_x\rangle - (1-b)\langle Y, N_{x,z}\rangle \\
a_3 &= \langle N_z, p_1\rangle + \langle N_x, p_2\rangle + \langle Y, p_3\rangle.
\end{aligned} \tag{28}$$

All $a_i$ occurring are positive for $w_a^{-1}$ and $w_p^{-1}$ smaller than one. The magnitudes are $a_1 \sim O(1)$, $a_2 \sim O(10)$ and $a_3 \sim O(10^3)$.

Equation (26) describes the dynamics of the director and the fluid velocity slightly above the threshold of the homogeneous instability:

$$\mathbf{n} = \mathbf{n}^0 + B\mathbf{n}^{\text{lin}}, \quad \mathbf{v} = \mathbf{v}^0 + B\mathbf{v}^{\text{lin}} \tag{29}$$

where $\mathbf{n}^{\text{lin}}$, $\mathbf{v}^{\text{lin}}$ is the solution of the linear problem (17) in physical units.

## 4. Results and comparison with experiment

Recent conoscopic observations of the nematic MBBA under steady shear flow [8] provide data for a comparison with theoretical results. Let us introduce a twist angle $\phi$ and a splay angle $\theta$ in the following way:

$$n_x = \cos\theta\cos\phi, \quad n_y = \cos\theta\sin\phi, \quad n_z = \sin\theta. \tag{30}$$

Then, the twist angle $\phi = \tan^{-1}(n_y/n_x)$ and the splay angle $\theta = \sin^{-1} n_z$. For small perturbations of the basic

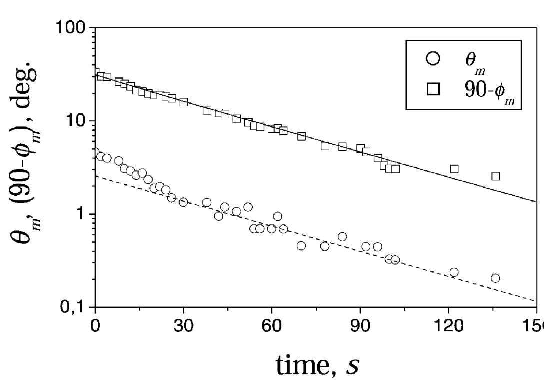


Figure 1. Twist and splay relaxation of the director. Symbols are experimental data from [8], solid and dashed lines are theoretical calculations for $90^\circ - \phi_m$ and $\theta_m$, respectively. Rigid boundary conditions are assumed in the calculations.

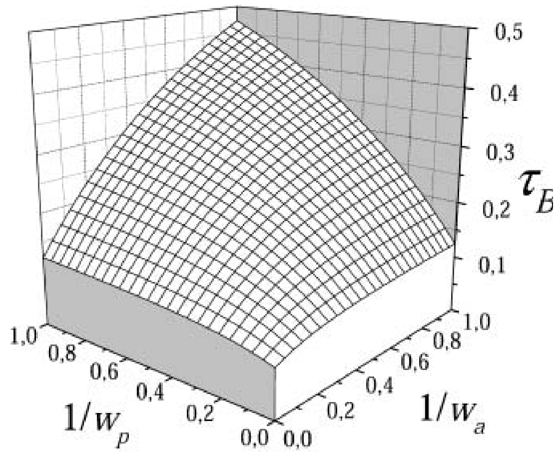


Figure 2. The (dimensionless) relaxation time $\tau_B$ (27) vs. anchoring strengths: $d = 150\,\mu m$, for material parameters of MBBA see [18].

state (4) one has

$$\pi/2 - \phi \approx \hat{n}_x\,,\ \theta \approx \hat{n}_z\,. \quad (31)$$

From the analysis of the conoscopic images it is possible to extract the angles $\phi_m = \phi(z=0)$ and $\theta_m = \theta(z=0)$ [21]. In figure 1 the twist and splay relaxation of the director after cessation of the shear flow with slightly supercritical shear rate is presented.‡ Symbols are experimental points from [8], lines are theoretical data calculated for rigid boundary conditions. Fitting of the experimental data to an exponential gives relaxation times $\tau_\phi \approx 46.0$ s and $\tau_\theta = 29.5$ s for $\phi_m$ and $\theta_m$, respectively (one can see in figure 1 that on the logarithmic scale the lines for $\phi_m$ and $\theta_m$ are not parallel, at least for initial times). The reason for the difference in twist and splay relaxation times is unclear. In the framework of the amplitude equation approach the time relaxation is the same for both components of the director (i.e. for both angles $\phi_m$ and $\theta_m$) and the velocity. From equations (27) and (28) it follows that for MBBA material parameters [18], the LC layer thickness $d = 150\,\mu m$ and strong anchoring for the director $\tau_B \approx 48.4$ s, which is in good agreement with the relaxation time of $\phi_m$.

It is interesting to investigate the ratio of the director component perturbations [or twist and splay angles due to expressions (31)], which is independent of the overcriticality $\epsilon$, since $\hat{n}_x$ and $\hat{n}_z$ are parts of the eigenvector of equation (15). Using equations (31) and (17) one has for the angles in the middle of the layer

$$\frac{\frac{\pi}{2}-\phi_m}{\theta_m} = \frac{1}{\beta}\left[\frac{1+m_p}{1-m_p} - \frac{w_a\cosh(a_c/2)+a_c\sinh(a_c/2)}{w_a}\cdot\frac{m_p+m_a}{1-m_p}\right]. \quad (32)$$

For rigid boundary conditions this ratio constitutes $\approx 11.7$, which is in good agreement with experimental data [8], giving $\approx 12$ for times $t > 30$ s (see figure 1). For weaker anchoring the ratio (32) slightly changes and approaches $\approx 12.6$ with $w_a$, $w_p \to 0$.

In contrast, the relaxation time $\tau_B$ appears to be strongly influenced by the anchoring strengths $w_a$ and $w_p$. Strong anchoring conditions give the lower limit for $\tau_B$. In figure 2 the dependence of $\tau_B$ on $w_a$ and $w_p$ is presented. The relaxation time increases with decreasing anchoring strengths and changes its magnitude by almost a factor of five in the range of $w_a$ and $w_p$ shown

‡An exact value of the critical shear rate is not reported in [8], but from the presented graphs it can be estimated by interpolating the data to be about 0.14–0.15 $s^{-1}$. From our calculations for the parameters of this experiment ($d = 150\,\mu m$, MBBA material parameters [18]) it follows that the critical shear rate is $\approx 0.19\,s^{-1}$.

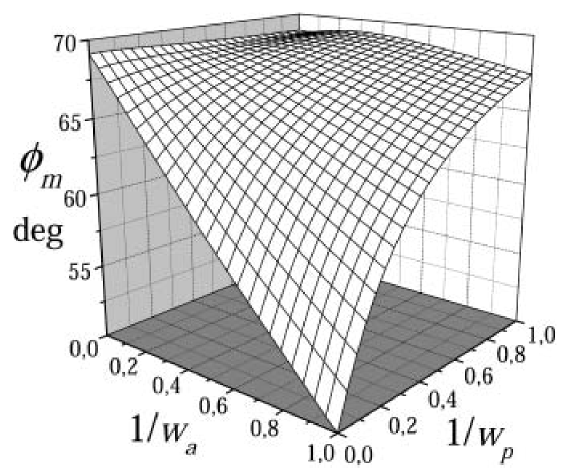


Figure 3. Twist angle $\phi_m$ vs. anchoring strengths for $\epsilon^2 = 0.1$: $d = 150\,\mu m$, for MBBA material parameters see [18].

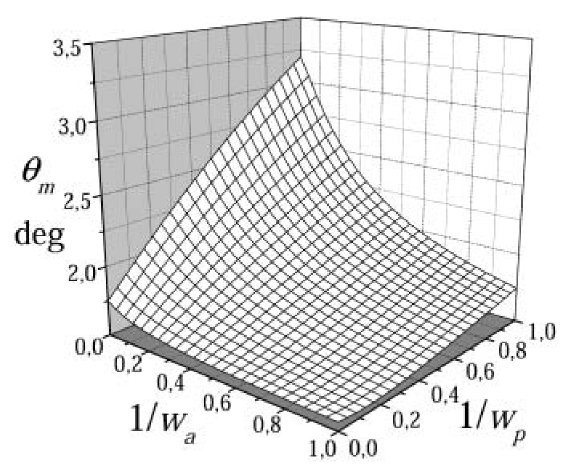


Figure 4. Splay angle $\theta_m$ vs. anchoring strengths for $\epsilon^2 = 0.1$: $d = 150\,\mu m$, for MBBA material parameters see [18].

in figure 2. Clearly, such a large variation of the relaxation time could easily be detected experimentally.

The stationary solutions of equation (26) can be used to calculate the orientation of the director for a given overcriticality $\epsilon$. These solutions have been studied by Manneville for strong anchoring conditions [12]. For the case of weak anchoring the turning angles $\phi_m$ and $\theta_m$ versus $w_a^{-1}$ and $w_p^{-1}$ are presented in figures 3 and 4, respectively. One can see that the twist angle $\phi_m$ for large $w_a$ and $w_p$ is mainly controlled by the azimuthal component $w_a$ of the anchoring strength: for large $w_a$ the angle $\phi_m$ remains almost unchanged as $w_p$ varies (figure 3). For the splay angle $\theta_m$ the situation is reversed (figure 4). The variation of the turning angles with the anchoring strengths is well pronounced.

## 5. Conclusions

The study of the relaxation of the perturbation amplitude after cessation of Couette flow with slightly overcritical shear rate presented here makes it clear that changes to the anchoring strengths $w_a$ and $w_p$ lead to strong variation of the relaxation time $\tau_B$. This effect can be used to obtain a reliable estimate of the anchoring strengths in addition to the effect of a reduction of the critical shear rate under weak anchoring conditions. Since $\tau_B$ is a monotonic function for each of $w_a$ and $w_p$ (see figure 2) it is sufficient to measure the relaxation time once in order to calculate both components of the anchoring force. The changes in the director turning angles $\phi_m$ and $\theta_m$ obtained by varying the anchoring strengths can also be used for experimental measurements of $w_a$ and $w_p$, although this effect is not as strong as in the case for the relaxation time $\tau_B$. In the practically important range $w_a^{-1}, w_p^{-1} < 0.25$ (for LC layer thickness $d = 150\,\mu m$) modern experimental techniques are powerful enough to resolve small variations (several degrees) of these angles with $w_a$ and $w_p$.

It is now known that for a slightly different set of LC material parameters the primary instability can change its type and become spatially periodic [16], which is analogous to the case of MBBA with a strong enough magnetic field applied perpendicular to the flow plane. This means that there exist two 'dangerous' modes with similar growth rates near the transition from one type of instability to another. It would be particularly interesting to investigate the orientational dynamics of a LC in a weakly non-linear regime in the region of these parameters by means of an extended weakly non-linear analysis [22]. This work is intended for the future.

Many useful discussions and help with the early stages of this work by Dr A.P. Krekhov and Prof. L. Kramer are gratefully acknowledged. The author would like to thank Alexei Krekhov for his critical reading of a draft of this paper and his many helpful comments on it; also H.H. Winter for providing electronic files with experimental data. Different parts of the research described here were supported by DAAD, grant A/97/53326, DFG, grant Kr690/14-1, RFBR, grant 02-02-17435 and the European graduate school 'Nonequilibrium Phenomena and Phase Transitions in Complex Systems' funded by DFG.

## References

[1] Bryan-Brown, G. P., Wood, E. L., and Sage, I. C., 1999, *Nature*, **399,** 338.
[2] Chigrinov, V. G., 1999, *Liquid Crystals Devices: Physics and Applications* (New York: Artech House).
[3] Ericksen, J. L., 1961, *Trans. Soc. Rheol.* **5**, 23; Leslie, F. M., 1968, *Arch. Ration. Mech. Anal.*, **28**, 265.
[4] Leslie, F. M., 1979, *Adv. Liq. Cryst.*, **4,** 1.
[5] Ericksen, J. L., 1966, *Arch. Ration. Mech. Anal.*, **23,** 266.
[6] Pieranski, P., and Guyon, E., 1974, *Phys. Rev. A*, **9,** 404.
[7] Pieranski, P., and Guyon, E., 1973, *Solid State Commun.* **13**, 435; Pieranski, P., and Guyon, E., 1976, *Commun. Phys*, **1**, 45.
[8] Boudreau, D. M., Winter, H. H., Lillya, C. P., and Stein, R. S., 1999, *Rheol. Acta*, **38,** 503.
[9] Manneville, P., and Dubois-Violette, E., 1976, *J. de Phys. (Fr.)*, **37,** 1115.
[10] Leslie, F. M., 1976, *J. Phys. D: appl. Phys.*, **9,** 925.
[11] Manneville, P., and Dubois-Violette, E., 1976, *J. de Phys. (Fr.)*, **37,** 285.
[12] Manneville, P., 1979, *J. de Phys. (Fr.)*, **40,** 713.
[13] Dubois-Violette, E., and Manneville, P., 1996, in *Pattern Formation in Liquid Crystals*, edited by A. Buka and L. Kramer (Berlin: Springer-Verlag), pp. 91–164.
[14] Tarasov, O. S., Krekhov, A. P., and Kramer, L., 2001, *Liq. Cryst.*, **28,** 833.
[15] Nasibullayev, I. Sh., Tarasov, O. S., and Krekhov, A. P. (to be published).
[16] Tarasov, O. S., 2003, PhD thesis, University of Bayreuth, Germany.
[17] Khazimullin, M. V., Börzsönyi, T., Krekhov, A. P., and Lebedev, Yu. A., 1999, *Mol. Cryst. liq. Cryst.*, **329,** 247.
[18] Kneppe, H., Schneider, F., and Sharma, N. K., 1982, *J. chem. Phys.* **77**, 3203; de Jeu, W. H., Claassen, W. A. P., and Spruijt, A. M. J., 1976, *Mol. Cryst. liq. Cryst.*, **37**, 269.
[19] Jérôme, B., 1991, *Rep. Prog. Phys.*, **54,** 391.
[20] Nicolis, G., 1995, *Introduction to Nonlinear Science* (Cambridge: University Press).
[21] Cladis, P. E., 1972, *Phys. Rev. Lett.*, **28,** 1629.
[22] Plaut, E., and Pesch, W., 1999, *Phys. Rev. E*, **59,** 1747.